JOC*Article*

7,11-*epi*-Thyrsiferol: Completion of Its Synthesis, Evaluation of Its Antimitotic Properties, and the Further Development of an SAR Model

Gisele A. Nishiguchi,[†] John Graham,[†,‡] A. Bouraoui,[§,⊥] R. S. Jacobs,[§] and R. Daniel Little*[,†]

Department of Chemistry and Biochemistry and Department of Ecology, Evolution, and Marine Biology, University of California, Santa Barbara, Santa Barbara, California 93106

little@chem.ucsb.edu

Received March 9, 2006

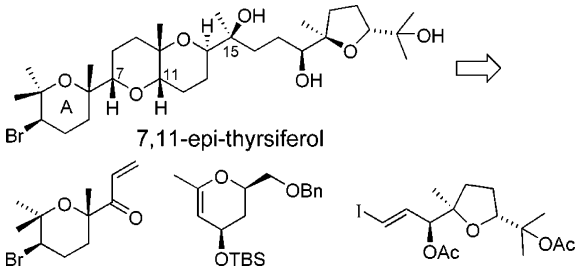

We (a) describe the completion of a total synthesis of 7,11-*epi*-thyrsiferol (**4**), (b) compare the antimitotic activities of thyrsiferol (**2**), $\Delta^{15,28}$-dehydrothyrsiferol (**3**), and 7,11-*epi*-thyrsiferol (**4**), (c) evaluate the synergistic behavior of the title compound and colchicine to inhibit cell proliferation, and (d) describe the results of conformational searches that provide additional insight concerning the SAR profile of the thyrsiferol family of natural products.

Introduction

The marine environment offers a diverse array of structures that provide significant challenges to the development of synthetic methodology. In addition, biologically active natural products present a unique opportunity to identify novel pharmacophores and provide a useful platform through which unidentified mechanisms of drug action can be revealed.[1]

Squalene-derived metabolites isolated from red algae of the genus *Laurencia* display a broad range of bioactivities.[2] We, and many others, have been particularly attracted to thyrsiferyl 23-acetate (**1**, Figure 1) and $\Delta^{15,28}$-dehydrothyrsiferol (**3**).[3] The former exhibits strong in vitro cytotoxic activities against the P388 (murine lymphoid neoplasm) mammalian cancer cell line,[4] and induces rapid apoptotic cell death in a variety of human T- and B-cell lines while displaying a selective inhibition of protein serine/threonine phosphatase 2A (PP2A), but not PP1, PP2B, and PP2C.[5]

In 2005 we described the titanium(III)-mediated coupling of **5** and **6** to assemble **7** (Scheme 1),[6] and identified the latter as a potentially useful intermediate for the synthesis of cis-fused

[†] Department of Chemistry and Biochemistry.

[‡] Recipient of a 2005 SOC Pfizer Summer Undergraduate Research Fellowship.

[§] Department of Ecology, Evolution, and Marine Biology.

[⊥] Fulbright Visiting Scholar; April 1, 2005 to September 30, 2005. Present address: Laboratory of Pharmacology, Faculty of Pharmacy, University of Monastir, Monastir 5000, Tunisia.

(1) (a) Faulkner, D. J. *Nat. Prod. Rep*. **2000**, *17* (1), 7−55. (b) Faulkner, D. J. *Nat. Prod. Rep*. **2000**, *17* (1), 1−6. (c) Lei, J.; Zhou, J. *J. Chem. Inf. Comput. Sci.* **2002**, *42*, 742−748. (d) Blunt, J. W.; Copp, B. R.; Munro, M. H. G.; Northcote, P. T.; Prinsep, M. R. *Nat. Prod. Rep.* **2004**, *21*, 1 and references therein.

(2) (a) Fernandez, J. J.; Souto, M. L.; Norte, M. *Nat. Prod. Rep.* **2000**, *17*, 235−246. (b) Suzuki, T.; Suzuki, M.; Furusaki, A.; Matsumoto, T.; Kato, A.; Imanaka, Y.; Kurosawa, E. *Tetrahedron Lett.* **1985**, *26*, 1329−1332. (c) Morimoto, Y.; Iwai, T.; Kinoshita, T. *J. Am. Chem. Soc*. **2000**, *122*, 7124−7125.

(3) (a) Isolation and characterization of thyrsiferol: Blunt, J. W.; Hartshorn, M. P.; McLennan, T. J.; Munro, M. H. G.; Robinson, W. T.; Yorke, S. C. *Tetrahedron Lett.* **1978**, *1*, 69−72. (b) Isolation and characterization of $\Delta^{15,28}$-dehydrothyrsiferol: Gonzalez, A. G.; Arteaga, J. M.; Fernandez, J. J.; Martin, J. D.; Norte, M.; Ruano, J. Z. *Tetrahedron* **1984**, *40* (14), 2751−2755. (c) Isolation and characterization of 10-*epi*-$\Delta^{15,28}$-dehydrothyrsiferol: Norte, M.; Fernandez, J. J.; Souto, M. L.; Garcia-Gravalos, M. D. *Tetrahedron Lett.* **1996**, *37* (15), 2671−2674.

(4) Suzuki, T.; Suzuki, M.; Furusaki, A.; Matsumoto, T.; Kato, A.; Inanaka, Y.; Kurosawa, E. *Tetrahedron Lett.* **1985**, *26* (10), 1329−1332.

(5) (a) Matsuzawa, S.; Suzuki, T.; Suzuki, M.; Matsuda, A.; Kawamura, T.; Mizuno, Y.; Kikuchi, K. *FEBS Lett.* **1994**, *356*, 272−274. (b) McCluskey, A.; Sim, A. T. R.; Sakoff, J. A. *J. Med. Chem.* **2002**, *45* (6), 1151−1175 and references therein.

(6) Nishiguchi, G. A.; Little, R. D. *J. Org. Chem*. **2005**, *70* (13), 5249−5256.

10.1021/jo060519z CCC: $33.50
Published on Web 06/30/2006

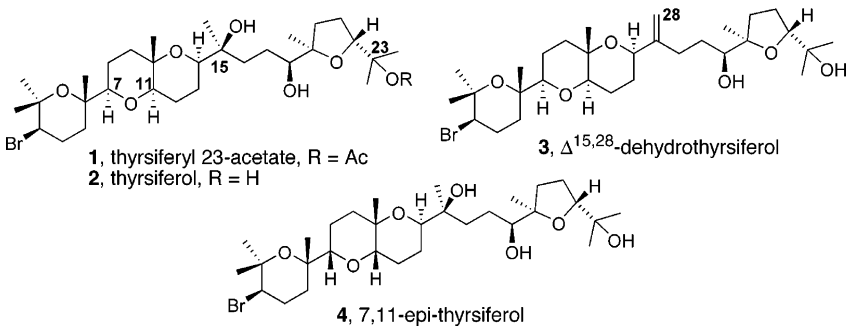

FIGURE 1. Thyrsiferol 23-acetate (**1**), thyrsiferol (**2**), $\Delta^{15,28}$-dehydrothyrsiferol (**3**), and 7,11-*epi*-thyrsiferol (**4**).

SCHEME 1. Synthetic Analysis for the Construction of 7,11-*epi*-Thyrsiferol (4)

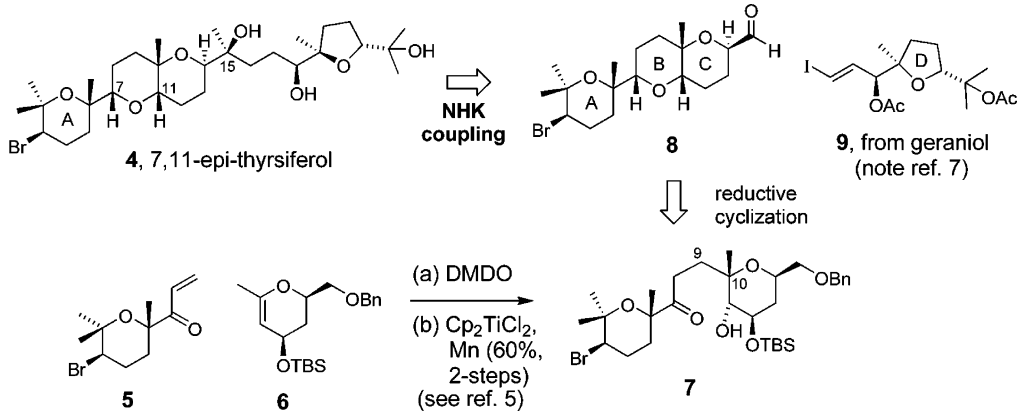

SCHEME 2. Completion of the Total Synthesis of 7,11-*epi*-Thyrsiferol (4)[a]

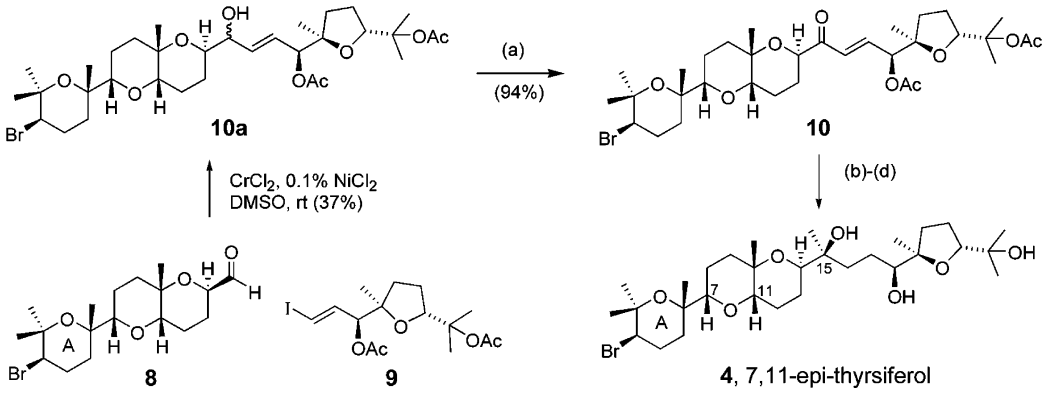

[a] Reagents and conditions: (a) Dess−Martin periodinane, CH_2Cl_2, $NaHCO_3$, rt (94%); (b) H_2, Pd/C, EtOAc, rt (90%); (c) MeMgBr, THF, 0 °C (81%); (d) K_2CO_3, MeOH, rt (78%).

analogues of thyrsiferol. We chose 7,11-*epi*-thyrsiferol (**4**) as our objective and describe herein the completion of its total synthesis as well as several aspects of its pharmacological profile (see below).

Synthesis. In addition to the Ti (III) mediated coupling reaction described previously, key features of the synthetic route include the reductive cyclization of **7** to generate the B-ring, and a Nozaki−Hiyama−Kishi (NHK) coupling of **8** with iodide **9** (see Scheme 1).[7] The iodide was conveniently prepared from geraniol according to a procedure published by Forsyth and coworkers.[8]

The NHK coupling was performed with $CrCl_2$ and 0.1% $NiCl_2$ in dry DMSO at room temperature. Under these mild conditions, a diastereomeric mixture of alcohols, **10a**, was obtained in a 37% yield (Scheme 2). Our objective at this stage was to complete the synthesis in order to obtain material for screening (vide infra). Consequently, we did not attempt to optimize the conversion. Oxidation with Dess Martin periodinane proceeded in a 94% yield to afford the α,β-unsaturated ketone **10**. Subsequent hydrogenation delivered the expected saturated ketone with 90% efficiency. A chelation-controlled addition of the methyl group to C_{15} was conveniently and efficiently achieved by using methylmagnesium bromide (81%). Finally, saponification of the acetate units with potassium

(7) (a) Takai, K.; Tagahira, M.; Kuroda, T.; Oshima, K.; Utimoto, K.; Nozaki, H. *J. Am. Chem. Soc.* **1986**, *108*, 6048. (b) Kress, M. H.; Ruel, R.; Miller, L. W. H.; Kishi, Y. *Tetrahedron Lett.* **1993**, *34*, 5999.

(8) (a) Gonzalez, I. C.; Forsyth, C. J. *Org. Lett.* **1999**, *1* (2) 319−322. (b) Gonzalez, I. C.; Forsyth, C. J. *J. Am. Chem. Soc.* **2000**, *122*, 9099−9108.

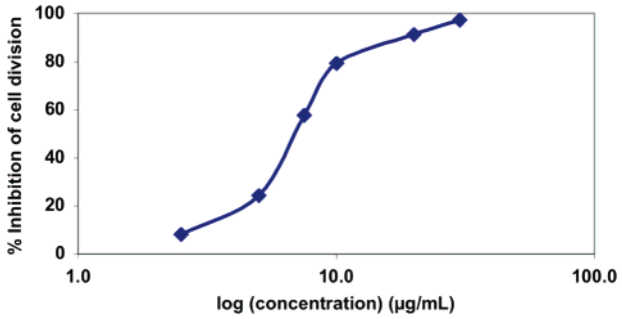

FIGURE 2. Log concentration response curve for inhibition of *S. purpuratus* first embryonic cell division by 7,11-*epi*-thyrsiferol (**4**, $IC_{50} \approx 7$ μg/mL).

carbonate in methanol afforded a 78% yield of the target structure, 7,11-*epi*-thyrsiferol (**4**). The overall sequence, *including* the preparation of the components **5**, **6**, and **9**, required 32 steps, the longest linear sequence being 17 steps. Completion of the total synthesis of 7,11-*epi*-thyrsiferol (**4**) provided us with an opportunity to investigate several features of its biological profile. The results are described below.

Pharmacological Investigations. We selected sea urchin embryos for the in vitro evaluation of antimitotic activity, since fertilized eggs of the species *Strongylocentrotus purpuratus* (hereafter referred to as *S. purpuratus*) constitute a system that is selective toward agents that disrupt mitotic spindle function, thereby facilitating the identification of potential anticancer agents.[9] Compared to mammalian cancer cell cultures, the sea urchin bioassay constitutes a practical and affordable alternative for screening antimitotic properties. The assay utilizes seawater as a culture medium and does not require sterile conditions. The embryos are simply incubated in a temperature regulated water bath (15 °C); the first cell division occurs shortly after fertilization (~120 min). Cell division is monitored in the presence of a potential drug. Inhibition of cell division is indicative of antimitotic activity. The fertilized eggs undergo many highly synchronous divisions so that a large number of specimens are easily obtained thereby facilitating a statistical analysis. This allows cell proliferation studies to be completed in the course of 1 day.

In this paper we report (1) the antimitotic activities of thyrsiferol (**2**), $\Delta^{15,28}$-dehydrothyrsiferol (**3**), and 7,11-*epi*-thyrsiferol (**4**); (2) the synergistic behavior of **4** and colchicine to inhibit cell proliferation; and (3) the results of conformational search calculations that were conducted to provide insight concerning structure and activity.

Antimitotic Activity of 7,11-*epi*-Thyrsiferol (4). A screen of the antimitotic activity of 7,11-*epi*-thyrsiferol (**4**) established that it inhibits the first cleavage of *S. purpuratus* embryo in a concentration dependent manner, with 50% inhibition (IC_{50}) occurring at approximately 7 μg/mL (11 μM; Figure 2). At a concentration of 30 μg/mL (48 μM), 100% inhibition of the first mitosis occurs; neither lysis nor morphological abnormalities were observed at any of the concentrations used.

The actions of thyrsiferol (**2**) and dehydrothyrsiferol (**3**) were determined under similar conditions for comparison. They too

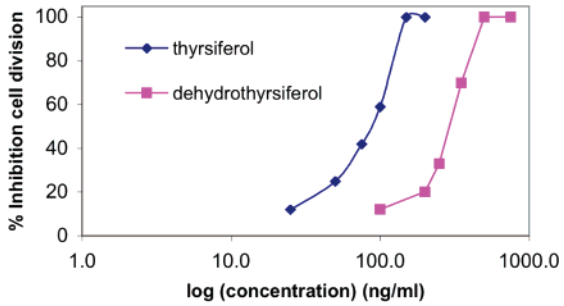

Compound	IC_{50}
thyrsiferol (**2**)	0.14 μM
dehydrothyrsiferol (**3**)	0.48 μM
7,11-*epi*-thyrsiferol (**4**)	11 μM

FIGURE 3. Log concentration response curve for inhibition of *S. purpuratus* embryo cleavage by thyrsiferol (**2**; $IC_{50} \approx 85$ ng/mL) and dehydrothyrsiferol (**3**; $IC_{50} \approx 280$ ng/mL) and summary of IC_{50} data.

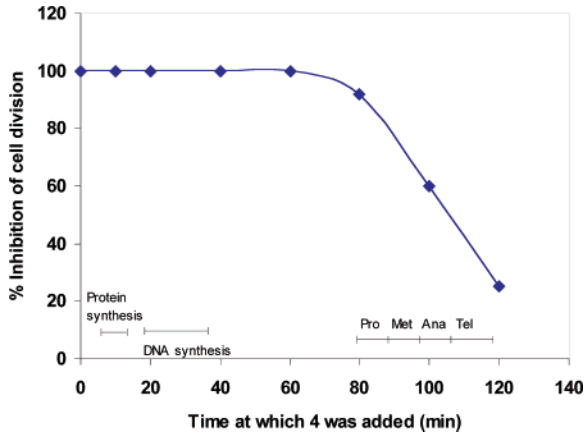

FIGURE 4. The effect of 7,11-*epi*-thyrsiferol (**4**) at different stages of the cell cycle in *S. purpuratus* embryos. Pro, Met, Ana, and Tel are abbreviations for prophase, metaphase, anaphase, and telophase of mitosis, respectively.

inhibited the first cleavage of *S. purpuratus* embryos in a concentration dependent manner, with 50% inhibition occurring at 85 ng/mL (0.14 μM) and 280 ng/mL (0.48 μM), respectively (Figure 3 and the accompanying table). Thus in the present assay, **2** and **3** are more potent than the synthetic analogue 7,-11-*epi*-thysiferol (**4**), with thyrsiferol (**2**) being the most potent of the three.

The effect of 7,11-*epi*-thyrsiferol (**4**) at different stages of the cell cycle was determined by adding an amount of it that was known to produce 100% inhibition of the first mitosis (viz., 30 μg/mL) at 10-min intervals after fertilization. In this manner, it was discovered that complete inhibition of embryonic cleavage continues to occur even when **4** is added as late as 70 min after fertilization, but declines steeply after 80 min. As illustrated in Figure 4, **4** proved effective through protein and DNA synthesis, as well as the prophase of the cell cycle.

Synergism between 7,11-*epi*-Thyrsiferol (4) and Colchicine. Colchicine is an antimitotic agent that is known to disrupt microtubule formation.[10] The simultaneous administration of 7,-11-*epi*-thyrsiferol (**4**) with colchicine promised to allow the detection of synergistic or additive effects upon the inhibition of cell division.

(9) (a) Jacobs, R. S.; Wilson, L. In *Modern Analysis of Antibiotics*; Aszalos, A., Ed.; Marcel Dekker: New York, 1986. (b) Nishioka, D.; Marcell, V.; Cunningham, M.; Khan, M.; Von Hoff, D. D.; Izbicka, E. In *Novel Anticancer Drug Protocols*; Methods in Molecular Medicine, Vol. 85; Buolamwini, J. K., Adjei, A. A., Eds.; Humana Press: Totowa, NJ, 2003; p 265.

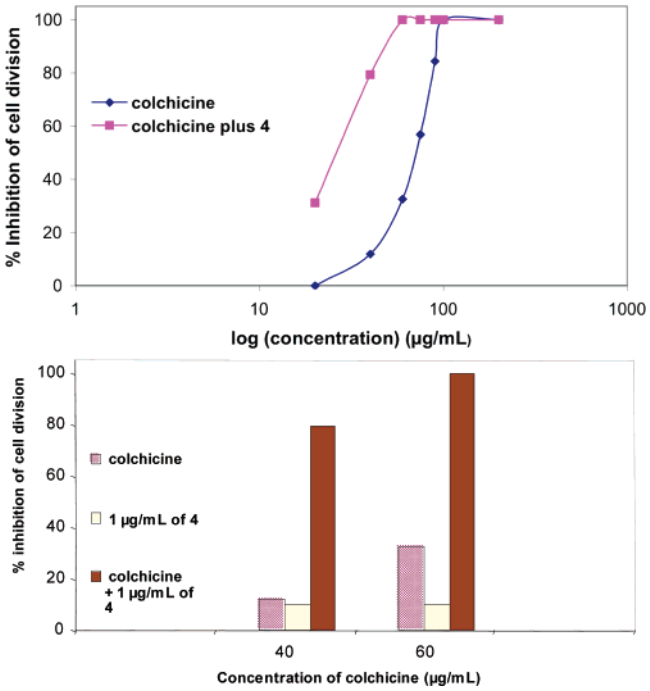

FIGURE 5. Synergy between colchicine and 7,11-*epi*-thyrsiferol (**4**). The combination of **4** with colchicine decreases the concentration of colchicine required to induce 50% inhibition of cell division in the sea urchin embryo.

As illustrated by the histograms portrayed in Figure 5, at a colchicine concentration of 40 μg/mL, ~10% of the cell division is inhibited. Alone, 7,11-*epi*-thyrsiferol (**4**) expresses approximately the same level of effectiveness at a concentration of 1 μg/mL. *When the two substances are combined*, a dramatic rise to ~70% inhibition is observed. Complete inhibition is achieved when the assay is conducted at [colchicine] ≥ 60 μg/mL and [7,11-*epi*-thyrsiferol] = 1 μg/mL. Moreover, in the presence of 7,11-*epi*-thyrsiferol (**4**), colchicine's IC_{50} is reduced more than 2-fold, from 70 μg/mL to 27 μg/mL. Clearly colchicine and **4** act synergistically to inhibit cell proliferation. This experiment supports our observation that compound **4** acts as a mitotic spindle poison. Additional studies are needed, however, to determine the precise mechanism by which it acts to inhibit cell proliferation.

Discussion

On the basis of extensive investigations, Fernandez, Souto, Norte, and co-workers have described some of the structural features that they believe are responsible for the bioactivity of thyrsiferol (**2**) and its analogues.[11,12] These include the need for a conformationally flexible chain appended to C_{14} of the tricyclic core; they also highlight the importance of having an hydroxyl group at either C_{15} or C_{16}, and suggest that the conformation of the $C_{15}-C_{19}$ side chain is at least partially responsible for the variation in biological responses among the analogues.

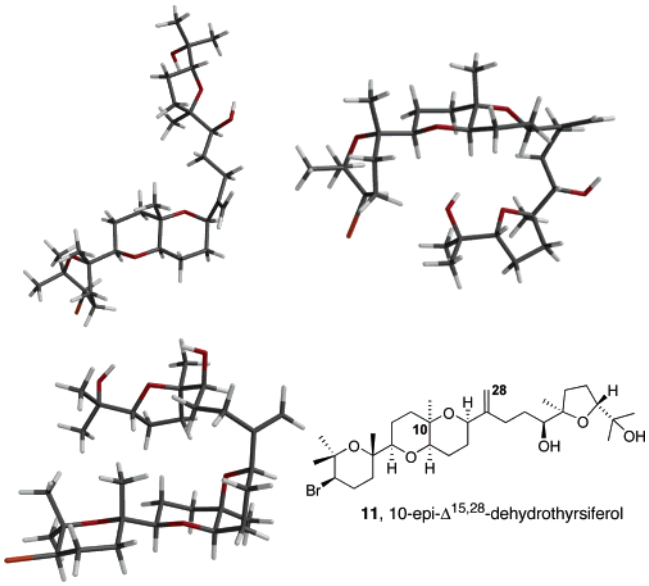

FIGURE 6. The two calculated lowest energy conformers for dehydrothyrsiferol (top), and the lowest energy conformer of 10-*epi*-$\Delta^{15,28}$-dehydrothyrsiferol (bottom).

These researchers have formulated a useful model that can easily be adapted to predict whether a newly synthesized substance like 7,11-*epi*-thyrsiferol (**4**) ought to be more or less active than thyrsiferol analogues whose bioactivity has been determined. The model is based upon the results of Monte Carlo conformational search calculations wherein distance constraints, obtained from NOESY spectral correlations, were imposed.[11] They suggest that the most potent structures are those where the $C_{15}-C_{19}$ chain is turned "downward" relative to the ABC core structure, while compounds with reduced potencies adopt geometries where the side chain turns "upward".[13]

Unlike Fernandez, Souto, and Norte, we did not obtain NOESY spectral data. Consequently, we were unable to include distance constraints in our calculations, and therefore, we did not anticipate precise agreement with their results. We did, however, anticipate agreement with the upward/downward sense of the side chain coiling; this proved to be the case.

Without constraints, we discovered that the two lowest energy conformers for dehydrothyrsiferol (**3**) differed by only 0.11 kcal/mol. In the lowest energy form, the chain is turned toward the "back" of the tricyclic core. This is clearly seen by viewing the structure from the top, as is illustrated on the left side of Figure 6. In the conformer that is 0.11 kcal/mol higher in energy, illustrated on the top right, the chain coils downward in accord with the findings of Norte and co-workers for the most active forms of the thyrsiferol analogues that they screened. In this instance, they determined that the IC_{50} for dehydrothyrsiferol (**3**) toward the P-388 cancer cell line was 0.017 μM. In contrast, 10-*epi*-$\Delta^{15,28}$-dehydrothyrsiferol (**11**; Figure 6, bottom) displayed a 100-fold decrease in potency toward the same cell line (IC_{50} of 1.7 μM). Like Fernandez, Souto, and Norte, we found that the side chain of the calculated lowest energy conformer for **11**

(10) (a) Taylor, A.; Mamelak, M.; Golbetz, H.; Maffly, R. *J. Membr. Biol.* **1978**, *40* (3), 213−235. (b) Malkinson, F. D. *Arch. Dermatol*. **1982**, *118*, 453−457. (c) Dumontet, C.; Sikic, B. *J. Clin. Oncol.* **1999**, *17* (3), 1061. (d) Hastie, S. B. *Pharmacol. Ther.* **1991**, *51*, 377−401.

(11) Fernandez, J. J.; Souto, M. L.; Norte, M. *Bioorg. Med. Chem.* **1998**, *6*, 2237−2243.

(12) Souto, M. L.; Manriquez, C. P.; Norte, M.; Leira, F.; Fernandez, J. J. *Bioorg. Med. Chem. Lett.* **2003**, *13*, 1261−1264.

(13) The conformers are viewed from a perspective where (a) the ABC core is oriented with the B and C rings roughly perpendicular to the page and approximately parallel to the horizontal, (b) the B ring pyran oxygen resides in front of the page, (c) the A ring is positioned on the left, and the side chain to the right, and (d) a "downward turn" signifies a clockwise turn of the $C_{15}-C_{19}$ chain relative to the ABC core, while an "upward turn" signifies a counterclockwise turn.

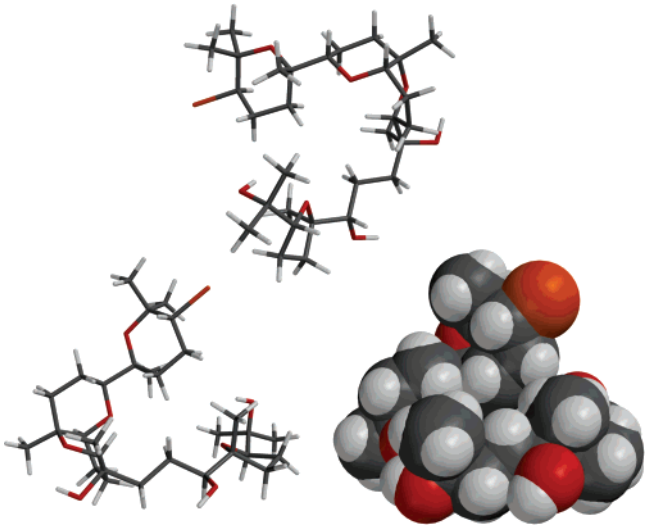

FIGURE 7. Two perspectives corresponding to the lowest energy conformation of 7,11-*epi*-thyrsiferol (**4**): top, illustrating the downward turn of the side chain; bottom, tube (left) and space-filling (right) renderings illustrating the polar perimeter and nonpolar core.

coiled upward, this in accord with their hypothesis that diminished bioactivity is correlated with an upward turn.

Encouraged by the agreement of our calculations with the published results, we felt sufficiently confident to explore the conformational space for the synthetic material, 7,11-*epi*-thyrsiferol (**4**). We were curious to determine whether it would adopt a conformation that more closely resembled dehydrothyrsiferol (**3**) or 10-*epi*-$\Delta^{15,28}$-dehydrothyrsiferol (**11**), and whether its conformation would be indicative of its modest biological activity in the sea urchin assay (vide supra). As was the case for the structures shown above, our calculations used the Monte Carlo conformational search program that is included in the SPARTAN software suite (viz., MMFFaq using the SM50R solvation model).[14]

Like dehydrothyrsiferol (**3**, $IC_{50} = 0.48\ \mu M$ in the sea urchin assay), the side chain appended to the B-ring of the lowest energy conformation for 7,11-*epi*-thyrsiferol (**4**) turns downward. This outcome is consistent with its modest bioactivity ($IC_{50} = 11\ \mu M$ in the sea urchin assay), and suggests that it would be more active than **11** in the same assay. The side chain of **3** coils downward, presumably to maximize van der Waals attractive forces on the underside, and also to ensure that the polar oxygen atoms are oriented toward the outside. These attributes are easily visualized in the space filling representation illustrated in Figure 7.

Concluding Remarks

The sea urchin bioassay proved to be a convenient and powerful means by which to assess aspects of the biological profile of the synthetic material 7,11-*epi*-thyrsiferol (**4**), and to define new profiles for thyrsiferol (**2**) and $\Delta^{15,28}$-dehydrothyrsiferol (**3**). The investigation revealed the antimitotic properties of these materials, and served to identify possible mechanistic pathways by which their activity is expressed. We feel that additional studies are warranted and will report the results of our investigations when they become available.

Experimental Section

Enone 10. To a solution of **8** (17 mg, 0.044 mmol) and **9** (45 mg, 0.110 mmol) in DMSO (2 mL), and maintained at room temperature under an argon atmosphere, was added $CrCl_2$ containing 0.5% $NiCl_2$ by weight (28 mg, 0.221 mmol). The mixture was stirred for 48 h and then quenched with 2 mL of a 1 M solution of potassium serinate (prepared by dissolving 0.84 g of serine and 0.6 g of $NaHCO_3$ in 7 mL of H_2O). Ethyl acetate (2 mL) was added and the mixture was stirred for 30 min. The layers were separated, and the aqueous phase was extracted with ethyl acetate (3 × 2 mL) and dried with Na_2SO_4. Concentration and column chromatography of the crude material (petroleum ether and diethyl ether: 1:1 by volume) afforded 11 mg (0.016 mmol, 37%) of the desired coupling product as a mixture of diastereomeric alcohols, **10a**. The mixture was dissolved in 1 mL of CH_2Cl_2 and $NaHCO_3$ (13 mg, 0.16 mmol) was added, followed by Dess−Martin periodinane (20 mg, 0.048 mmol). The reaction was allowed to stir for 1 h, then quenched with ethyl acetate (2 mL), saturated aqueous $NaHCO_3$ (2 mL), and 10% aqueous $Na_2S_2O_3$ (2 mL). The resulting solution was stirred for 30 min, the aqueous phase was extracted with ethyl acetate (3 × 2 mL), and the combined organic mixtures were washed with brine, dried over $MgSO_4$, filtered, and concentrated under reduced pressure to give an oil. Column chromatography of the crude material with petroleum ether and diethyl ether (1:1) afforded 10 mg of the desired enone product (0.015 mmol, 94%). Its spectral data were the following: ^{1}H NMR ($CDCl_3$, 400 MHz) δ 6.97 (dd, J = 16.0, 4.9 Hz, 1H), 6.71 (dd, J = 16.0, 1.5 Hz, 1H), 5.43 (dd, J = 4.9, 1.5 Hz, 1H), 4.36 (m, 1H), 4.10 (dd, J = 8.4, 6.3 Hz, 1H), 3.88 (dd, J = 12.4, 4.1 Hz, 1H), 3.22 (m, 1H), 3.05 (dd, J = 11.2, 2.0 Hz, 1H), 2.27 (qd, J = 13.2, 3.8 Hz, 1H), 2.16 (s, 3H), 1.99 (s, 3H), 1.47 (s, 3H), 1.45 (s, 6H), 1.41−2.1 (m, 15H), 1.33 (s, 3H), 1.30 (s, 3H), 1.21 (s, 3H), 0.95 (s, 3H). ^{13}C NMR ($CDCl_3$, 100 MHz) δ 201.0, 170.4, 169.9, 141.2, 127.0, 85.4, 84.1, 83.5, 82.5, 77.2, 76.1, 75.4, 75.0, 74.9, 70.7, 58.9, 37.6, 34.3, 31.3, 30.9, 28.0, 26.4, 25.0, 24.2, 23.5, 23.5, 22.5, 22.4, 22.1, 21.7, 21.0, 20.0, 17.4. IR (neat) 2926, 1736, 1233, 1033. HRMS (ESI) calcd for $C_{33}H_{51}O_9NaBr$ 693.2608, found 693.2596.

Conversion of 10 to 7,11-*epi*-Thyrsiferol (4): (a) Saturation of Enone C═C π-Bond. To a room-temperature solution of enone **10** (10 mg, 0.015 mmol) in 1 mL of EtOAc was added 5 mg of Pd/C (10%). The mixture was stirred for 3 h under an atmosphere of H_2 (balloon). The polarity of both starting material and product are very similar by TLC. After 3 h, the solution was filtered through a pad of Celite, then washed with 10 mL of EtOAc; the filtrate was concentrated and the crude material was chromatographed with petroleum ether and diethyl ether (3:2 by volume) to afford a clear, colorless oil corresponding to the desired ketone (9 mg, 0.013 mmol, 90%). ^{1}H NMR ($CDCl_3$, 400 MHz) δ 4.90 (dd, J = 10.1, 3.0 Hz, 1H), 4.31 (dd, J = 6.9, 5.0 Hz, 1H), 4.02 (dd, J = 9.2, 6.0 Hz, 1H), 3.87 (dd, J = 12.4, 4.1 Hz, 1H), 3.28 (m, 1H), 3.04 (dd, J = 11.1, 2.0 Hz, 1H), 2.83 (ddd, J = 18.2, 9.7, 6.1 Hz, 1H), 2.52 (ddd, J = 18.1, 9.7, 5.2 Hz, 1H), 2.25 (qd, J = 13.2, 4.0 Hz, 1H), 2.08 (s, 3H), 1.98 (s, 3H), 1.35−1.95 (m, 13H), 1.46 (s, 3H), 1.44 (s, 3H), 1.43 (s, 3H), 1.32 (s, 3H), 1.29 (s, 3H), 1.21 (s, 3H), 0.95 (s, 3H). ^{13}C NMR ($CDCl_3$, 100 MHz) δ 212.8, 170.7, 170.5, 85.1, 84.3, 83.6, 82.5, 77.3, 76.4, 75.9, 75.0, 74.9, 70.4, 58.9, 37.3, 34.8, 34.1, 31.3, 30.9, 28.0, 26.4, 25.7, 24.1, 23.8, 23.6, 22.9, 22.7, 22.4, 21.7, 21.1, 20.1, 19.2. IR (neat) 2975, 1737, 1370, 1236. HRMS (ESI) calcd for $C_{33}H_{53}O_9NaBr$ 695.2765, found 695.2775.

(b) Grignard Addition. The resulting ketone (6 mg, 0.0089 mmol) was dissolved in 0.8 mL of anhydrous THF and cooled to

(14) The Monte Carlo conformational searches were conducted by using the MMFFaq force field of the Spartan '04 Macintosh software package. The search routine randomly explores conformational space, beginning at a temperature that is sufficient to ensure that the system does not get stuck in a local minimum, and gradually decreasing as more conformers are explored. Conformers whose energies are > 10.0 kcal/mol above the lowest energy conformer are discarded. Once the minimizations were completed by using the MMFF force field, the SM50R solvation model was applied to each conformer in an effort to simulate the presence of water.

−78 °C under an argon atmosphere. MeMgBr (3.1 M solution in diethyl ether, 30 μL, 0.11 mmol) was added dropwise and the mixture was stirred at −78 °C for 1 h. The reaction mixture was quenched with saturated NH_4Cl (1 mL), and the aqueous layer was extracted with ethyl acetate (3 × 2 mL), washed with brine (5 mL), dried with $MgSO_4$, and concentrated. Silica gel column chromatography with petroleum ether and ethyl acetate (3:1) afforded the desired product as a clear, colorless oil (5 mg, 0.007 mmol, 81%). ^{1}H NMR ($CDCl_3$, 400 MHz) δ 4.90 (dd, J = 9.8, 3.2 Hz, 1H), 4.01 (dd, J = 9.1, 6.0 Hz, 1H), 3.95 (dd, J = 10.9, 5.1 Hz, 1H), 3.87 (dd, J = 12.4, 4.0 Hz, 1H), 3.37 (dd, J = 5.2, 1.4 Hz, 1H), 3.01 (dd, J = 10.9, 2.3 Hz, 1H), 2.46 (br s, 1H), 2.25 (qd, J = 13.2, 3.8 Hz, 1H), 2.08 (s, 3H), 1.99 (s, 3H), 1.25−1.98 (m, 19H), 1.46 (s, 3H), 1.44 (s, 3H), 1.43 (s, 3H), 1.32 (s, 3H), 1.29 (s, 3H), 1.21 (s, 3H), 1.12 (s, 3H), 1.07 (s, 3H). ^{13}C NMR ($CDCl_3$, 100 MHz) δ 170.8, 170.4, 84.9, 84.3, 83.5, 82.5, 78.3, 77.3, 75.7, 75.0, 74.8, 73.0, 70.0, 58.8, 37.3, 34.2, 32.6, 31.3, 30.9, 28.0, 27.1, 26.4, 24.1, 23.8, 23.6, 23.4, 23.1, 22.9, 22.5, 22.4, 21.7, 21.2, 20.1, 18.8. IR (neat) 2933, 1737, 1370, 1237. HRMS (ESI) calcd for $C_{34}H_{57}O_9$-NaBr 711.3078, found 711.3090.

(c) Removal of the Acetates: 7,11-*epi*-Thyrsiferol (4). In 0.5 mL of MeOH was dissolved 1.5 mg of the above alcohol (0.0022 mmol) at room temperature under argon. Potassium carbonate (1.0 mg, 0.0044 mmol) was added and the reaction was stirred for 5 h. The solvent was removed in vacuo and the crude material was chromatographed with petroleum ether and ethyl acetate (1:1) to afford the final material as a clear oil (**4**, 1.0 mg, 0.0017 mmol, 75%). ^{1}H NMR ($CDCl_3$, 500 MHz) δ 3.98 (m, 1H), 3.88 (dd, J = 12.4, 4.0 Hz, 1H), 3.77 (dd, J = 9.7, 6.0 Hz, 1H), 3.45 (d, J = 10.0, 1.7 Hz, 1H), 3.38 (dd, J = 5.1, 1.4 Hz, 1H), 3.02 (dd, J = 10.9, 2.3 Hz, 1H), 2.27 (qd, J = 12.3, 3.8 Hz, 1H), 1.23−2.38 (m, 19H), 1.44 (s, 3H), 1.31 (s, 3H), 1.30 (s, 3H), 1.22 (s, 3H), 1.17 (s, 3H), 1.15 (s, 3H), 1.14 (s, 3H), 1.10 (s, 3H). ^{13}C NMR ($CDCl_3$, 125 MHz) δ 87.4, 86.0, 83.5, 77.8, 77.2, 76.8, 76.3, 76.1, 75.0, 74.8, 73.3, 58.8, 37.2, 33.9, 32.5, 31.5, 31.0, 28.1, 27.7, 27.2, 26.6, 25.6, 24.1, 24.0, 23.6, 23.3, 23.3, 23.1, 20.2, 18.9. IR (neat) 3415, 2923, 1372, 1128. HRMS (ESI) calcd for $C_{30}H_{53}O_7$NaBr 627.2866, found 627.2888.

Inhibition of Cell Cleavage in Sea Urchin Embryo. Sea urchins, *Strongylocentrotus purpuratus*, were induced to spawn by injecting 0.5 M KCl into the coelomic cavity. The eggs were maintained in filtered seawater (13−15 °C) while spermatozoa were collected undiluted from the aboral surface of male sea urchins and stored on ice. Eggs were then passed through a 150 mm Nitex filter, three times, to remove the jelly coating that covers the eggs and hinders fertilization. The eggs were then resuspended in freshly filtered seawater at a concentration of approximately 1% (v/v) and the sperm were diluted in seawater (1 drop of concentrated sperm per 1 mL of seawater).

Eggs were fertilized by adding diluted sperm solutions to the diluted egg suspensions (1 mL of sperm suspension per 100 mL of diluted egg suspension) and were then added to various synthetic or natural product concentrations dissolved in 10 μL of DMSO. The embryos were then incubated in a controlled-temperature water bath at 15 °C for approximately 120 min after fertilization.

The embryos were fixed in a 10% formaldehyde solution after the control embryo had progressed to the end of the first cleavage; quantification of cell division was performed visually by using light microscopy. Approximately 300 divided and nondivided embryos were counted per replicate. The percent inhibition of cell division was calculated relative to vehicle (DMSO) controls.

The effect of **4** at different stages of the cell cycle was determined by adding it, at 10-min intervals after fertilization, to aliquots of sea urchin embryos. The percentage inhibition of the first cleavage corresponds to the ratio of the number of undivided cells compared to the number of divided cells.

Synergism between 4 and Colchicine. The antimitotic activity of colchicine (Sigma-Aldrich) was determined separately, in the absence and in the presence of **4**. In the first instance, 1 mL of fertilized eggs was added to various concentrations of colchicine (20, 40, 60, 75, 90, 100, and 200 μg/mL) dissolved in 10 μL of DMSO. In the second case, 10 μg of **4** was added to various concentrations of colchicine and then 1 mL of fertilized eggs was added to the combined products. The embryos were then incubated at 15 °C in a water bath for approximately 120 min after fertilization.

Monte Carlo Conformational Searches. The Monte Carlo conformational searches were conducted with use of the MMFFaq force field of the Spartan '04 Macintosh software package. In each instance, more than 1800 conformers were sampled and their energies were determined. The lowest energy conformer is illustrated in the text. The search routine randomly explores conformational space, beginning at a temperature that is sufficient to ensure that the system does not get stuck in a local minimum, and gradually decreasing as more conformers are explored. Conformers whose energies are >10.0 kcal/mol above the lowest energy conformer are discarded. Once the minimizations were completed with the MMFF force field, the SM50R solvation model was applied to each conformer in an effort to simulate the presence of water.

Acknowledgment. We are grateful to the Cancer Research Coordinating Committee (CRCC) of the University of California for a grant that funded a portion of this research. G.A.N. thanks the Tokuyama family of Santa Barbara, CA, for a fellowship. A.B. acknowledges, with thanks, the Fulbright Foundation for a fellowship that allowed him to study in R.S.J.'s laboratory at UCSB. J.G. gratefully acknowledges Pfizer for their support of his participation in the SURF Program during the summer of 2005. The authors thank Professor M. Norte for samples of the natural products thyrsiferol and dehydrothyrsiferol that were used in the pharmacological investigations.

Supporting Information Available: ^{1}H and ^{13}C NMR spectra for compounds are available for aldehyde **8** and the conversion of **10** to **4**. This material is available free of charge via the Internet at http://pubs.acs.org.

JO060519Z